Fibril Breaking Accelerates α-Synuclein Fibrillization

Volodymyr V. Shvadchak[†,‡,], Mireille M.A.E. Claessens[‡], Vinod Subramaniam[†,‡,*]*

[†]FOM Institute AMOLF, Science Park 104, 1098 XG Amsterdam, The Netherlands

[‡]Nanobiophysics, MESA+ Institute for Nanotechnology & MIRA Institute for Biomedical Technology and Technical Medicine, University of Twente, PO Box 217, 7500 AE Enschede, The Netherlands

ABSTRACT

The formation of amyloid fibrils of α-synuclein (αSyn), the key protein in Parkinson's disease, is an autocatalytic process that is seeded by mature αSyn fibrils. Based on systematic measurements of the dependence of the fibril growth rate on the concentrations of monomers and preformed fibrillar seeds, we propose a mechanism of αSyn aggregation that includes monomer binding to fibril ends and secondary nucleation by fibril breaking. The model explains the increase of the αSyn aggregation rate under shaking conditions and the exponential increase in the fraction of fibrillar protein at the initial stages of αSyn aggregation. The proposed autocatalytic mechanism also accounts for the high variability in the aggregation lag time. The rate constant of monomer binding to the ends of fibrils, $k_+ \approx 1.3\ mM^{-1}s^{-1}$, was estimated from the aggregation rate and previously reported average fibril lengths. From the aggregation rates at low concentrations the binding of monomeric αSyn to fibrils was found to be almost irreversible, with an equilibrium dissociation constant (K_d) smaller than 3 μM.

KEYWORDS: Amyloid, aggregation, mechanism, autocatalytic reaction, kinetics.

INTRODUCTION

α-Synuclein (αSyn) is a 140 residue long intrinsically disordered protein that plays a key role in Parkinson's disease. It is highly expressed in the brain[1,2] and is predominantly localized at neuronal terminals.[1,3] Individuals having either additional copies of the gene coding for αSyn or disease-related single amino-acid substitutions in αSyn[4] have an increased risk to develop Parkinson's disease. Neurons affected by the disease present characteristic inclusions rich in αSyn amyloid fibrils.

Amyloid fibrils exhibit ordered cross β-sheet structure and are generally thermodynamically more stable than their respective monomers. At high protein concentrations fibrils form spontaneously[5] and grow several microns long[6]. For many amyloid proteins, including αSyn,[7,8] fibrils grow by sequential binding of monomers to fibril ends. New amyloid fibrils can be formed by several mechanisms[9,10] including monomer oligomerization,[11] fibril breaking[12,13] or monomer-fibril interactions.[14]

The aggregation kinetics of αSyn is sensitively dependent on solution conditions[8] and is characterized by a very low sample-to-sample reproducibility of lag times. Under shaking conditions αSyn aggregates much faster than in quiescent conditions.[15] Interaction of αSyn with surfaces[16] or the air-water interface[17] can increase the rate of initial aggregate formation but does not change the general autocatalytic kinetic behavior.[18] The mechanism of αSyn aggregation has been the subject of numerous studies[7,8,17,19] but the rate-limiting steps and the role and nature of intermediates[19-21] are not well understood. Therefore, in biophysical studies the aggregation of αSyn is mostly described by empirical parameters, namely the lag time and the observed exponential growth rate.[22] Generalized analytical descriptions of amyloid fibril formation kinetics were recently proposed[23,24] but no particular mechanism was assigned to αSyn aggregation.[8]

In this work we aim to arrive at a quantitative description of seeded and unseeded aggregation of αSyn under both quiescent and shaking conditions, and to shed light on the details of the aggregation mechanism. We first explore the dependence of the aggregation rate of αSyn on the concentration of seeds and monomers and demonstrate that fibrillization occurs by reversible addition of monomers to fibril ends. Second, by varying protein concentration and shaking conditions we found that new fibrillization centers are formed predominantly by a fibril breaking mechanism. Finally we show that the rate constant of fibril elongation can be calculated based on the measured kinetic parameters and the average fibril length. This rate constant quantifies the fibrillization propensity and, in contrast to the lag time, is not sensitive to the agitation conditions. The fibril elongation rate constant has the potential to be a useful figure of merit in characterizing the details of αSyn amyloid growth mechanisms and in assessing the effect of inhibitors on amyloid fibril growth.[25,26]

EXPERIMENTAL METHODS

αSyn expression and purification

Protein preparation and purification was performed as described earlier.[27] Briefly, expression was performed in *E.coli* Bl21(DE3) transformed with the pT7-7 plasmid carrying the wt αSyn gene. Culturing in LB medium with 100 μg/ml ampicillin. After IPTG induction (1 mM, 4 h) bacterial cell pellets were harvested by centrifugation (6000 × g, 10 min) and resuspended in 10 mM Tris–HCl, pH 8.0, 1 mM EDTA and 1mM PMSF (10% of the culture volume) and stirred for 1 hour at 4 °C. Cells were lysed by sonication for 2 min and centrifuged (10000 × g, 20 min, 4 °C).

DNA was precipitated by adding streptomycin sulfate (1%, 15 min, 4 °C) and removed by centrifugation at 13500 × g for 30 min. Then αSyn was salted-out from the solution by slow addition of 0.295 g/ml of ammonium sulfate and mild stirring for 1 hour at 4 °C. Precipitated

protein was collected by centrifugation (13500 × g, 30 min, 4 °C). The pellet was gently resuspended in 10 mM Tris–HCl, pH 7.4 (5% of the culture volume) and filtered through a 0.22 μm filter. The solution was purified on a 6 ml ResourceQ column using an Äkta Purifier system (GE Healthcare). The protein was eluted using a linear gradient of NaCl (0–500 mM) in 10 mM Tris–HCl, pH 7.4 at a flow-rate of 3 ml/min. Collected fractions were checked for αSyn using SDS–PAGE. Fractions containing αSyn were pooled and concentrated (Vivaspin-20, 10 kDa; GE Healthcare). The sample was desalted with a PD-10 column (GE Healthcare) using 10 mM Tris–HCl pH 7.4 and diluted with Tris–HCl, pH 7.4 to a concentration of 250 μM. Aliquots of 0.5 ml were stored at −80 °C. Protein concentration was determined by the Tyr absorption at 275 nm using ε=5 600 M^{-1} cm^{-1}.

Kinetic measurements

Aggregation experiments were performed using a Tecan Infinite M200pro plate reader and monitored by Thioflavin T (ThT) fluorescence. All experiments were performed at 37 °C, with shaking (orbital, 6 mm amplitude, 142 rpm) in 96-well plates ("Nunc", Thermo Fisher Scientific) sealed with film ("Viewseal" Greiner Bio One) to avoid evaporation, using a volume of 125 μL per well. The final solution used for aggregation contained 6 mM Na-PO_4 buffer at pH 7.2, 150 mM NaCl, 9 mM NaN_3, 1 mM EDTA (to remove divalent ions bound to αSyn), and 5 μM ThT (≥ 5% of αSyn concentration). Protein concentration was 100 μM unless otherwise indicated.

Fluorescence of ThT was recorded from the bottom of the plate. Excitation was at 446 nm, emission at 485 nm, excitation and emission slits were 9 and 20 nm, respectively. Dependence of the final ThT signal on the initial αSyn concentration was linear for αSyn concentrations in the range 10-50 μM.

During experiments in quiescent conditions ThT fluorescence was read every 600s. Under shaking conditions measurements were performed every 370 s (300 s shaking and 70 s reading time). To quantify the effect of shaking on the αSyn aggregation we monitored it with constant time step but varied the fraction of time between measurement points during which the protein solution was shaken. The shaking time fraction, in contrast to changing the shaking amplitude or speed, should linearly correlate with the average number of fibril breaking events per second. For the shaking time fraction experiments 370 s measurement cycles included 70 s reading and variable shaking and quiescent times (for example shaking time fraction 0.28 means that during the 370s cycle, the sample was shaken for 120 s).

Seeds were prepared by combining three to five separately aggregated 100 μM αSyn samples that had reached the plateau of ThT fluorescence (mentioned in the text as "intact fibrils") and the concentration was assumed to be equal to the initial protein concentration. For preparation of "sonicated seeds" 200 to 500μL of the stock fibril solutions prepared as above were placed in 1.5 mL Eppendorf tubes and sonicated for 300 s in a water bath sonicator (VWR 75D ultrasonic cleaner, power 90W, bath volume 2.5L), without filtration or other contact with external material. All mixing was performed within 15 min before the start of measurements. When possible, samples were prepared by serial dilutions with seeds added just before the pipetting into separate wells.

The initial aggregation rate was determined by measuring the increase of the ThT signal within the first 3000 s of the measurements and then converted to μM s^{-1} using the intensity of ThT fluorescence for completely aggregated 50 μM αSyn. Measurements were typically started ~15 min after adding seeds to the protein solution. The aggregation rate in the exponential part of the curve (k_{EXP}) was determined as the rate of increase of the logarithm of ThT fluorescence intensity, using the range corresponding to monomer conversion below 30%. $k_{EXP}=(\ln(0.3)-\ln(0.02))/(t_{30\%}-t_{2\%})$ where $t_{30\%}$ and $t_{2\%}$ are the times needed for 30% and

2% monomer conversion to fibrils respectively. For experiments with >1 mol.% of seeds, we used $t_{30\%}$ and $t_{5\%}$.

RESULTS AND DISCUSSION

Aggregation of αSyn is an autocatalytic process. To monitor the formation of αSyn fibrils we added to the protein solution Thioflavin T (ThT), a commonly-used reporter dye that shows an increase in fluorescence upon binding to amyloids.[28] In accordance with numerous previous reports, we observe sigmoidal aggregation curves (Figure 1a). After a lag time, the fluorescence intensity starts to grow exponentially and subsequently slows down upon monomer depletion. Addition of a small amount (1 mol.%) of αSyn fibrils to the solution of protein monomers ("seeding") abrogates the lag time (Figure 1a) and strongly increases the initial fibrillization rate. In the absence of seeds, after the lag time the fraction of fibrillized αSyn increases exponentially up to ~30% conversion of the monomer (Figure 1a, lower panel). Such behavior could be explained by an autocatalytic process where the rate of the fibrillization is proportional to the amount of formed fibrils. Exponential growth of the fibrillar protein fraction and seeding of the aggregation by preformed fibrils is observed both with shaking and non-shaking (quiescent) conditions (Figure S3a), showing that fibril-dependent acceleration of aggregation is a key part of the αSyn fibrillization mechanism.

αSyn fibrils grow by monomer addition to fibril ends. Since αSyn fibrillization is autocatalytic and depends strongly on the concentration of fibrils we first studied the elongation of αSyn amyloid fibrils in the presence of a known amount of pre-formed fibrils (“seeds”). We measured the dependence of the initial aggregation rate on the concentration of monomer and of seeds.

When seeding conditions are constant the aggregation rate increases linearly with monomer concentration (Figure 1b). Since the fibril growth rate is linearly proportional to the αSyn

concentration, fibril elongation mostly occurs by binding of monomeric αSyn and not of protein oligomers.

At fixed monomer concentration the initial aggregation rate is linearly proportional to the concentration of seeds (Figure 1c). We compared seeding efficiencies of intact equilibrium fibrils and of the same weight concentration of sonicated fibrils. Upon sonication, intact fibrils with average lengths of about 1 μm break into shorter fibril fragments of approximately 50 nm (see Figure S4). Short sonicated fibrils were about 25-fold more efficient than long intact fibrils at the same weight concentration (Figure 1d, Figure S4) pointing to the dependence of the reaction rate on the concentration of fibril ends.

Therefore, the rate of fibril elongation is k_+[M][E], where [M] and [E] are the concentrations of monomers and fibril ends respectively, and can effectively be treated as a bimolecular reaction between fibril ends and monomeric protein in solution.

Reversibility. The binding of monomers to fibril ends is probably a reversible process and the dissociation rate is proportional to concentration of fibril ends. Since experiments show fibril growth, the monomer binding rate (k_+[M][E]) should be considerably higher than the dissociation rate (k_-[E]). The effective fibril elongation rate can be described by

$$d[\mathrm{F}]/dt = k_+[\mathrm{M}][\mathrm{E}] - k_-[\mathrm{E}] = k_+([\mathrm{M}]-K_d)\,[\mathrm{E}] \qquad \text{Eq. (1)}$$

where $K_d = k_-/k_+$ is the affinity constant of αSyn monomers to fibril ends, and [F] is the concentration of fibrillized protein, expressed as equivalent monomer concentration. This binding constant can be determined from the dependence of the initial fibrillization rate on the monomer concentration (Figure 1b) at constant seed concentration. A linear fit of the kinetic data to Eq. (1) yields a $K_d \sim 4\pm3$ μM for the affinity of αSyn monomers to fibril ends (Figure 1c), in good agreement with the previously reported threshold concentration of αSyn necessary for aggregation (> 2 μM)[5]. Aggregation of diluted αSyn solutions performed in the

presence of a constant fraction of 1 mol.% of sonicated αSyn fibrils shows protein fibrillization at 3 μM concentration (Figure S1) supporting that $K_d \leq 3$ μM.

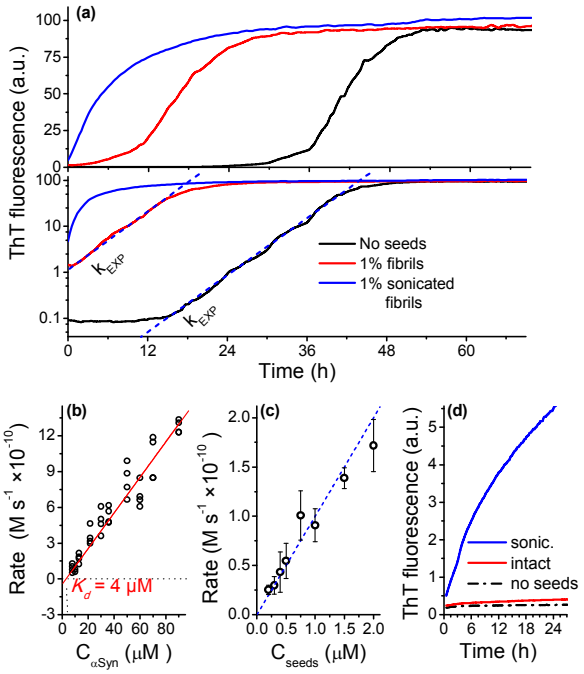

Figure 1. (a) Aggregation of αSyn in the absence of seeds (black), in the presence of 1 mol.% of intact mature fibrils (red) or 1 mol.% of sonicated fibrils (blue), monitored by ThT fluorescence depicted on linear (top) and logarithmic (bottom) scales. Curves are averages of 10 samples. Parallel blue dashed lines show that rate of exponential growth (k_{EXP}) is equal in the presence and absence of seeds. (b) The initial rate of αSyn aggregation at different αSyn concentrations, 200 nM of sonicated seeds. The red line is a linear fit to the equation $r=a\cdot(C_{\alpha Syn}-K_d)$. (c) Initial aggregation rate at different concentrations of sonicated seeds (expressed as monomer concentration). Error bars are the SD of 5 measurements. Dashed line is a guide to the eye. (d) Aggregation of αSyn in quiescent conditions in the presence of 0.2 mol.% sonicated (blue) or intact (red) fibrils as seeds. Curves are averages of 6 samples. The αSyn concentration was 50 μM in all experiments. Shaking at 142 rpm (a)-(c) or quiescent conditions (d).

Secondary nucleation. The exponential growth of the fibrillar αSyn fraction at early stages of the aggregation implies an exponential increase in the rate of αSyn fibrillization. The rate is proportional to the product of the monomer concentration and the concentration of fibril ends. Since the monomer concentration always decreases during the aggregation process, the increase of fibril formation rate is determined by the formation of new fibril ends. The observed exponential increase of the fibrillar protein fraction is possible only when new fibril ends are formed by a fibril-dependent mechanism with rate proportional to the amount of fibrils already present in solution ($d[E]/dt \sim [F]$). Formation of new growing centers dependent on the presence of fibrils is called "secondary nucleation" and is common for amyloid fibrillization.[9,29] The secondary nucleation can occur by monomer-independent fibril breaking or by a monomer-dependent mechanism.[9] The two possible mechanisms differ by sensitivity of the reaction rate to concentration of monomer. The exponential growth of the fibrillar αSyn fraction could be characterized by an apparent rate constant (k_{EXP}) equal to the slope of the kinetic curve in logarithmic scale (Figure. 1a).

In the case of fibril breaking the apparent rate constant (k_{EXP}) is expected to be proportional to the square root of the monomer concentration, while if monomers are included in the secondary nucleation step, k_{EXP} would increase proportionally to [M] or faster.[9] Aggregation of 10-100 μM αSyn in shaking conditions both in the absence of seeds and when seeded by a small amount of intact αSyn fibrils shows apparent rates approximately proportional to $[M]^{½}$ (Figure 2b). The slope of the graph in logarithmic scale (Figure 2b, inset), yields $d(\ln k_{EXP})/d(\ln[M])=0.6\pm0.1$ (Figure S3), which is consistent with a secondary nucleation mechanism involving fibril breaking.

The notion of a fibril breaking mechanism is also supported by a strong increase of the aggregation rate upon mechanical agitation. Fibrils of αSyn are of micrometer lengths and

can, in contrast to nanometer-sized monomers and oligomers, be expected to be more susceptible to breakage by mechanical and shear forces induced by agitation of the solution.

Since the concentration of αSyn fibrils increases exponentially with time, the rate of formation of new fibril ends is linearly proportional to the total amount of the fibrillized protein

$$d[\mathrm{E}]/dt = k_b[\mathrm{F}] \qquad \text{Eq. (2)}$$

where k_b is the breaking rate constant per unit fibril length (i.e. one protein molecule). We assume here that a fibril can break with equal probability at any position, and should lead to an exponential length distribution of the fibrils (see SI for derivation), which has been observed experimentally (ref.[6], Figure 2c).

Mechanism. The simplest mechanism that explains such an autocatalytic fibrillization of αSyn includes three steps (Figure 2a):

1) ***Initiation***: Monomers (M) form initial fibrils with active growing ends (E);
2) ***Growth***: Monomers bind fibril ends increasing the amount of fibrillar αSyn (F);
3) ***Formation of new fibril ends*** from existing fibrils (secondary nucleation).

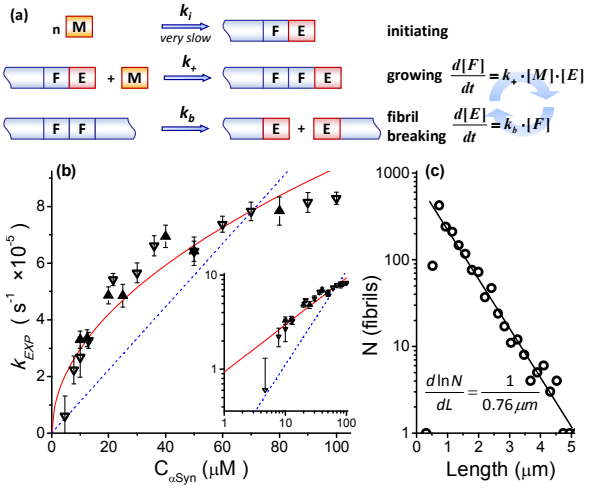

Figure 2. (a) Kinetic scheme of fibrillization. M, E and F are αSyn molecules in solution, in the fibril ends, and in the internal part of fibrils respectively. (b) The rate of the exponential part of the αSyn aggregation at different monomer concentrations. The red solid line is the fit to the model described in the text and the blue dashed line corresponds to the monomer-dependent nucleation model.[14] Open and closed triangles are results of two independent experiments (including protein purification and seed preparation). Insert shows the same graph in log scale. The aggregation was seeded by 1 mol.% of intact fibrils (~1μm long). (c) The distribution of lengths of αSyn fibrils based on the data from ref.[6] Experiment was performed at continuous shaking and 100 μM αSyn concentration. Due to the sample preparation procedure the number of fibrils of length <500 nm is probably underestimated in this data set.

The frequency of fibril breaking events is proportional to the total amount of fibrillar protein. On the other hand, the rate of fibrillization is proportional to the amount of fibril ends that creates a positive feedback loop necessary for an autocatalytic process and consequently an exponential increase of fibrillar αSyn.

The combination of equations (1) and (2) describes the evolution of αSyn fibril content during the aggregation after formation of initial fibrils. Numerical solution of the system of equations yields curves that fit the experimental aggregation data well (Figure S6). An analytical solution is challenging but a very good analytical approximation that describes the curve, except for the last stages, was recently obtained.[23,30]

The behavior of the system in the early and late stages of the aggregation process can be conveniently described separately.

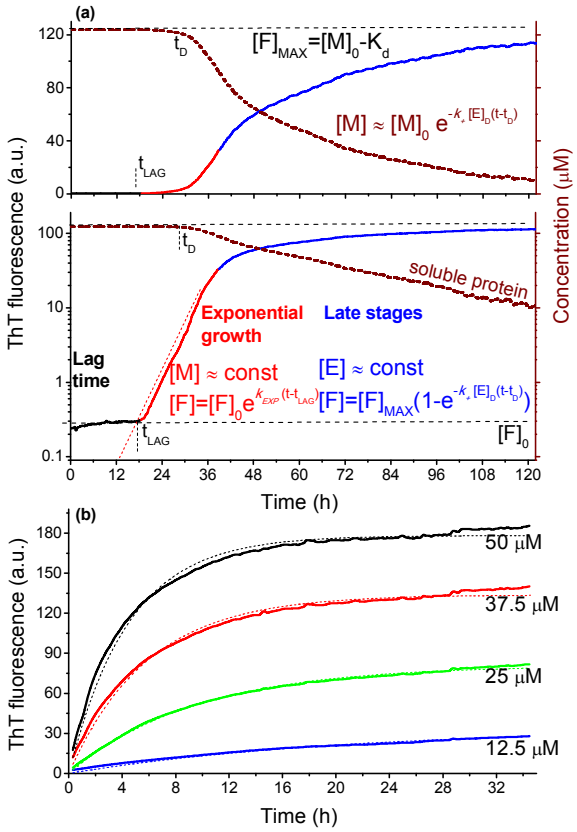

Figure 3. (a) Changes of ThT fluorescence during different stages of αSyn fibrillization in linear (top) and logarithmic (bottom) scales. Brown dashed line corresponds to the calculated amount of the free monomer in solution estimated from a difference between the maximal signal and the observed signal. 50 μM αSyn aggregation under shaking conditions. (b) Aggregation of 12.5 to 50 μM αSyn seeded by 1 mol.% of sonicated fibrils performed under

shaking conditions. Averages of 6 experiments. Dashed lines are global fits to Eq. (4) resulting in parameters $k_+[E]_0 = C_{seeds} \cdot 1.25 \times 10^{-4}$ s^{-1} and $K_d = 2$ μM ($R^2 = 0.998$).

Early stages of the aggregation. For low and moderate conversion of monomers to fibrils, the monomer concentration can be assumed constant ($[M] \approx [M]_0$). Then the combination of Eq.(1) and Eq.(2) yields (See SI for detailed derivation):

$$d^2[F]/dt^2 = k_+ k_b ([M]_0 - K_d)[F]$$

$$d(\ln[F])/dt = \pm\sqrt{k_+ k_b ([M]_0 - K_d)}$$

The observed exponential increase of the fibril content is described by the positive solution:

$$[F] = [F]_0 e^{t\sqrt{k_+ k_b ([M]-K_d)}} = [F]_0 e^{k_{EXP} t} \qquad \text{Eq. (3)}$$

where $[F]_0$ is the fibril concentration at t=0. The observed aggregation rate constant in the exponential phase is therefore $k_{EXP} = d\ln[F]/dt = (k_+ k_b([M]-K_d))^{1/2}$ that fits the experimental data, and shows a dependence proportional to the square root of the monomer concentration (Figure 2b). The same equation is valid also for aggregation seeded by intact fibrils (Figure 1a, red curve) as long as the total amount of fibrillar protein is lower than 30% (i.e. in the exponential stage).

Late stages of the aggregation. After fast growth of the fibrillar protein fraction described by Eq. (3), the rate of the aggregation decreases due to monomer depletion and becomes very similar to first order reaction kinetics (Figure 1, 3a). The rate of monomer depletion from solution is equal to the rate of fibril elongation:

$$d[M]/dt = -d[F]/dt = -k_+([M] - K_d)[E]$$

At late stages of the aggregation the monomer concentration is low and its relative changes are more significant than the changes of concentration of growing centers. Therefore the rate of aggregation mostly depends on the monomer concentration and concentration of fibril ends

could be considered constant ($[E] \approx [E]_D$). In such an approximation the fibril growth could be described by a first-order kinetic curve.

$$d([M]-K_d)/dt = -k_+[E]([M]-K_d)$$
$$[M] = K_d + const \cdot e^{-k_+[E]_D t}$$
$$[F] = ([M]_0 - K_d)(1 - e^{-k_+[E]_D (t-t_D)}) \qquad \text{Eq. (4)}$$

where $[M]_0$ is the initial monomer concentration and $[E]_D$ is the concentrations of fibril ends at time t_D (Figure 3a).

Aggregation of αSyn in the presence of excess of seeds is also described by Eq.(4). Such a situation is observed upon seeding of αSyn by sonicated fibrils that are about 25-fold shorter than intact preformed fibrils[8] (Figure S4) and yielding a commensurately large amount of fibril ends. The relatively high concentration of fibril ends remains approximately constant and the fibrillization rate decreases proportionally to the monomer concentration (Figure 3b).

Dependence on shaking. It has been widely reported that mechanical shaking increases the rate of αSyn aggregation.[31] In quiescent conditions αSyn seeded by intact fibrils shows a slow linear increase of the fibrillar protein fraction, while agitation of the samples leads to the exponential growth of fibril content (Figure 4a). Such an observation is consistent with the assumption of secondary nucleation by fibril breaking. Without shaking, fibril breaking is very slow, and the fibril growth rate is proportional to the initial seed concentration. Shaking increases the rate of fibril breaking, yielding an increase in the number of growing centers and therefore leads to the exponential growth of the fibrillar protein fraction. The rate of αSyn aggregation seeded by sonicated fibrils does not significantly depend on the shaking because the amount of growing centers present at the beginning of the reaction is significantly higher than the amount of new centers formed by fibril breaking (Figure 4a).

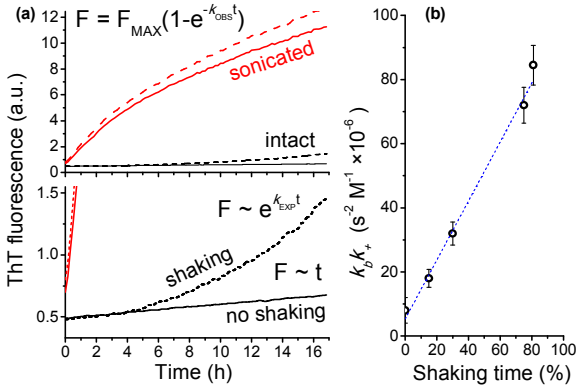

Figure 4. (a) Aggregation of αSyn in shaking (dashed) and quiescent (solid) conditions seeded by sonicated (red) or intact (black) fibrils. The bottom panel is a zoom-in of the top panel. (b) Dependence of the product of fibril breaking and fibril elongation rate constants (k_+k_b) on the shaking time fraction. Values were calculated as average k_{EXP}^2/[M] at αSyn concentrations of 100, 50, 25 and 12.5 μM, 5 repeats of each sample.

To quantify the effect of the fibril breaking rate on the αSyn aggregation we monitored it with constant time step (6 min) but varied the fraction of time between measurement points during which the protein solution was shaken. The shaking time fraction, in contrast to changing the shaking amplitude or speed, should linearly correlate with the average number of fibril breaking events per second. We observed that the square of the observed aggregation rate at the exponential stage was linearly proportional to the shaking time fraction (Figure 4b) and therefore to the average rate constant of fibril breaking in good agreement with Eq. (3). In quiescent conditions the rate of fibril breaking was more than 10-fold smaller than upon continuous shaking at 142 rpm with 6 mm amplitude.

It is very likely that the efficiency of fibril breaking upon shaking and therefore the aggregation rate would be dependent on the geometry and volume of the sample and presence of the water-air interface.[17]

Lag time and primary nucleation. The proposed autocatalytic mechanism requires the presence of an initial growing center that could be added to the system ("seeding") or formed by protein oligomerization. In the absence of seeds, the exponential increase of the ThT signal starts only after the so-called lag time. Lag time (t_{lag}) could be defined as the time at which the concentration of fibrils reaches a detectable level (Figure 3a). It is very likely that the concentration of fibrillar protein increases exponentially also before it reaches detectable levels, and that such a process starts from the appearance of the first fibrils.

The observed lag time has two components: the time necessary for formation of the first fibrils (t_{NUCL}) and the time required to amplify this amount until it is detectable using a ThT fluorescence assay: $t_{LAG}=t_{NUCL}+const/k_{EXP}$. The distribution of lag times is centered at a time point shifted from zero due to the delay between appearance of the first fibrils and the increase of the fibrillar αSyn concentration to a level above the instrumental detection threshold (Figure S10). The observed decrease of the lag times for aggregation under shaking conditions compared to quiescent conditions is therefore more likely attributable to faster growth of the fibrillar protein content by the autocatalytic mechanism than to a faster rate of primary nucleation. The lag times of αSyn aggregation show very high sample-to-sample variability that is much higher than the variability of the maximal aggregation rate or of the final fluorescence intensity. For aggregation under shaking conditions the lag times significantly decrease with increase of the sample volume (Figure S11). Increase of the sample volume at constant well geometry does not affect the rate of frequent processes occurring in solution or on the surfaces but only decreases the average time necessary to observe the first stochastic event in the system, for example formation of the first fibril growth center or the first fibril breaking event.

Length of fibrils. The average length of formed fibrils is proportional to the polymerization degree, that is, the number of αSyn molecules inside the fibrils divided by the

number of fibril ends (<*N*>=[F]/[E]). In the presence of excess of seeds the average number of monomers per fibril would be determined by the ratio of the initial concentrations of protein and of growing ends, so the maximal polymerization degree would be <N> = $[M]_0/[E]_0$ or $([M]_0-K_d)/[E]_0$ when taking into account that the aggregation would stop when the monomer concentration would decrease to K_d.

In the absence of seeds, or if they are not in excess and secondary nucleation dominates, both the number of fibrils and fraction of fibrillar protein increase exponentially with time. The polymerization degree of fibrils formed in such conditions is determined by the ratio of the fibril growth and fibril breaking rates:

$$< N >= \frac{d[F]/dt}{d[E]/dt} = \frac{k_+[E]([M]-K_d)}{k_b[F]}$$

Taking into account that [F]=<N>[E] this expression yields

$$< N >= \sqrt{k_+([M]-K_d)/k_b}$$

so that the average length of fibrils is approximately proportional to the square root of the monomer concentration in good agreement with previously published observations[6].

Rate constants. The experimentally observed rate of the exponential increase of fibrillar protein content depends on the product of fibril elongation (k_+) and breaking (k_b) rate constants: $k_{EXP} = \sqrt{k_+ k_b([M]-K_d)}$. Since fibril breaking strongly depends on the shaking intensity, k_{EXP} could be directly used for comparing experiments in different conditions. The protein fibrillization propensity is better described by the rate constant of monomer binding to fibril ends (k_+). Measurements of aggregation curves at different protein concentrations allow calculation of the product k_+k_b, but not of the individual constants. Additional information needed to determine the two rate constants separately could be obtained from the average length of fibrils formed during the exponential phase of the aggregation. Indeed, polymerization degree is determined by the ratio k_+/k_b: $< N >= \sqrt{([M]-K_d)k_+/k_b}$. The

product of the observed reaction rate and the polymerization degree does not depend on the fibril breaking rate $<N>k_{EXP}=k_+([M]-K_d)$. Therefore the rate of monomer binding to the fibril end could be calculated as

$$k_+ = \frac{< N > k_{EXP}}{[M] - K_d}$$

The average length of αSyn fibrils formed upon shaking is 1±0.5 μm (Figure 2c, ref.[6]). One monomer corresponds to 0.47 nm fibril length[32] therefore the polymerization degree of such fibrils $<N>\approx 2000\pm1000$. Combining this value with the observed exponential aggregation phase rate constant $k_{EXP}=6.5\cdot10^{-5}$ s^{-1} obtained with 50 μM αSyn (Figure 2b) we estimate $k_+=1.3\pm0.7$ mM^{-1}s^{-1}. The rate constant value corresponds to the addition of monomers to a specific fibril end approximately every 8 s at 100 μM αSyn concentration. This result agrees well with the value recently calculated from the initial rate of the seeded αSyn aggregation[8] (2 mM^{-1}s^{-1}) and with the average fibril growth rate of 1.4 nm/min measured in single fibril experiments.[7]

The rate constant obtained for αSyn is orders of magnitude lower than the reported fibril extension rates for other amyloidogenic proteins and peptides including Aβ[14] (~3000 mM^{-1}s^{-1}), prion protein[12] (200 mM^{-1}s^{-1}) and β2-microglobulin (72 mM^{-1}s^{-1}).[33] The slower rate of αSyn binding to fibrils compared to Aβ and prions is probably connected to the larger size of the protein and a correspondingly lower probability to adopt β-sheet conformation and bind the fibril end upon collision in solution.

CONCLUSIONS

Our data show that at physiological salt concentrations and upon shaking, the rate of αSyn amyloid fibril formation is determined by the secondary nucleation occurring by a fibril breaking mechanism. Fibrils grow by almost irreversible (K_d <3 μM) addition of monomers

to ends. Protein oligomers likely play a significant role only before the formation of the first fibrils.

A three-step autocatalytic fibrillization mechanism including nucleation, monomer addition, and fibril breaking accounts for distinctive features of the fibrillization process. These include the exponential growth of the fibril concentration at the beginning of (seeded) aggregation, the linear dependence of the observed aggregation rate constant on the square root of monomer concentration and the strong acceleration of aggregation by shaking. This model provides a quantitative means to compare αSyn aggregation rates and affinity to fibril ends under different conditions, and could be useful in characterizing and designing aggregation inhibitors.

ASSOCIATED CONTENT

Supporting Information. Supplementary figures and mathematical derivations. This material is available free of charge via the Internet at http://pubs.acs.org.

AUTHOR INFORMATION

Corresponding Authors

*Email: shvadchak@amolf.nl; subramaniam@amolf.nl.

Notes

The authors declare no competing financial interests.

ACKNOWLEDGMENT

We thank Ine Segers-Nolten for the raw data from ref.[6] used for the calculation of fibril length distributions, and Nathalie Schilderink and Kirsten van Leijenhorst-Groener for protein purification. This work is supported by NanoNextNL, a consortium of the Government of the Netherlands and 130 partners. VS also acknowledges support by "Stichting voor Fundamenteel Onderzoek der Materie" (FOM) as part of the FOM program titled "A Single Molecule View on Protein Aggregation".

REFERENCES

(1) Bendor, J. T.; Logan, T. P.; Edwards, R. H. The function of α-synuclein. *Neuron* **2013**, *79*, 1044-1066.

(2) Iwai, A.; Masliah, E.; Yoshimoto, M.; Ge, N.; Flanagan, L.; de Silva, H. A.; Kittel, A.; Saitoh, T. The precursor protein of non-Aβ component of Alzheimer's disease amyloid is a presynaptic protein of the central nervous system. *Neuron* **1995**, *14*, 467-475.

(3) Fortin, D. L.; Troyer, M. D.; Nakamura, K.; Kubo, S.; Anthony, M. D.; Edwards, R. H. Lipid rafts mediate the synaptic localization of α-synuclein. *J. Neurosci.* **2004**, *24*, 6715-6723.

(4) Polymeropoulos, M. H.; Lavedan, C.; Leroy, E.; Ide, S. E.; Dehejia, A.; Dutra, A.; Pike, B.; Root, H.; Rubenstein, J.; Boyer, R.; Stenroos, E. S.; et al. Mutation in the α-synuclein gene identified in families with Parkinson's disease. *Science* **1997**, *276*, 2045-2047.

(5) Baldwin, A. J.; Knowles, T. P.; Tartaglia, G. G.; Fitzpatrick, A. W.; Devlin, G. L.; Shammas, S. L.; Waudby, C. A.; Mossuto, M. F.; Meehan, S.; Gras, S. L.; et al. Metastability of native proteins and the phenomenon of amyloid formation. *J. Am. Chem. Soc.* **2011**, *133*, 14160-14163.

(6) van Raaij, M. E.; van Gestel, J.; Segers-Nolten, I. M.; de Leeuw, S. W.; Subramaniam, V. Concentration dependence of α-synuclein fibril length assessed by quantitative atomic force microscopy and statistical-mechanical theory. *Biophys. J.* **2008**, *95*, 4871-4878.

(7) Pinotsi, D.; Buell, A. K.; Galvagnion, C.; Dobson, C. M.; Kaminski Schierle, G. S.; Kaminski, C. F. Direct observation of heterogeneous amyloid fibril growth kinetics via two-color super-resolution microscopy. *Nano Lett.* **2014**, *14*, 339-345.

(8) Buell, A. K.; Galvagnion, C.; Gaspar, R.; Sparr, E.; Vendruscolo, M.; Knowles, T. P.; Linse, S.; Dobson, C. M. Solution conditions determine the relative importance of nucleation and growth processes in α-synuclein aggregation. *Proc. Natl. Acad. Sci. U S A* **2014**, *111*, 7671-7676.

(9) Cohen, S. I.; Vendruscolo, M.; Dobson, C. M.; Knowles, T. P. From macroscopic measurements to microscopic mechanisms of protein aggregation. *J. Mol. Biol.* **2012**, *421*, 160-171.

(10) Ruschak, A. M.; Miranker, A. D. Fiber-dependent amyloid formation as catalysis of an existing reaction pathway. *Proc. Natl. Acad. Sci. U S A* **2007**, *104*, 12341-12346.

(11) Sabareesan, A. T.; Udgaonkar, J. B. Amyloid fibril formation by the chain B subunit of monellin occurs by a nucleation-dependent polymerization mechanism. *Biochemistry* **2014**, *53*, 1206-1217.

(12) Collins, S. R.; Douglass, A.; Vale, R. D.; Weissman, J. S. Mechanism of prion propagation: amyloid growth occurs by monomer addition. *PLoS Biol* **2004**, *2*, e321.

(13) Meyer, V.; Dinkel, P. D.; Rickman Hager, E.; Margittai, M. Amplification of Tau fibrils from minute quantities of seeds. *Biochemistry* **2014**, *53*, 5804-5809.

(14) Cohen, S. I.; Linse, S.; Luheshi, L. M.; Hellstrand, E.; White, D. A.; Rajah, L.; Otzen, D. E.; Vendruscolo, M.; Dobson, C. M.; Knowles, T. P. Proliferation of amyloid-beta42 aggregates occurs through a secondary nucleation mechanism. *Proc. Natl. Acad. Sci. U S A* **2013**, *110*, 9758-9763.

(15) Giehm, L.; Otzen, D. E. Strategies to increase the reproducibility of protein fibrillization in plate reader assays. *Anal. Biochem.* **2010**, *400*, 270-281.

(16) Rabe, M.; Soragni, A.; Reynolds, N. P.; Verdes, D.; Liverani, E.; Riek, R.; Seeger, S. On-surface aggregation of α-synuclein at nanomolar concentrations results in two distinct growth mechanisms. *ACS Chem. Neurosci.* **2013**, *4*, 408-417.

(17) Campioni, S.; Carret, G.; Jordens, S.; Nicoud, L.; Mezzenga, R.; Riek, R. The presence of an air-water interface affects formation and elongation of α-synuclein fibrils. *J. Am. Chem. Soc.* **2014**, *136*, 2866-2875.

(18) Vacha, R.; Linse, S.; Lund, M. Surface effects on aggregation kinetics of amyloidogenic peptides. *J. Am. Chem. Soc.* **2014**, *136*, 11776-11782.

(19) Lorenzen, N.; Nielsen, S. B.; Buell, A. K.; Kaspersen, J. D.; Arosio, P.; Vad, B. S.; Paslawski, W.; Christiansen, G.; Valnickova-Hansen, Z.; Andreasen, M.; et al. The role of stable α-synuclein oligomers in the molecular events underlying amyloid formation. *J. Am. Chem. Soc.* **2014**, *136*, 3859-3868.

(20) Fauerbach, J. A.; Yushchenko, D. A.; Shahmoradian, S. H.; Chiu, W.; Jovin, T. M.; Jares-Erijman, E. A. Supramolecular non-amyloid intermediates in the early stages of α-synuclein aggregation. *Biophys. J.* **2012**, *102*, 1127-1136.

(21) Cremades, N.; Cohen, S. I.; Deas, E.; Abramov, A. Y.; Chen, A. Y.; Orte, A.; Sandal, M.; Clarke, R. W.; Dunne, P.; Aprile, F. A.; et al. Direct observation of the interconversion of normal and toxic forms of α-synuclein. *Cell* **2012**, *149*, 1048-1059.

(22) Morris, A. M.; Watzky, M. A.; Finke, R. G. Protein aggregation kinetics, mechanism, and curve-fitting: a review of the literature. *Biochim. Biophys. Acta.* **2009**, *1794*, 375-397.

(23) Knowles, T. P.; Waudby, C. A.; Devlin, G. L.; Cohen, S. I.; Aguzzi, A.; Vendruscolo, M.; Terentjev, E. M.; Welland, M. E.; Dobson, C. M. An analytical solution to the kinetics of breakable filament assembly. *Science* **2009**, *326*, 1533-1537.

(24) Hong, L.; Qi, X.; Zhang, Y. Dissecting the kinetic process of amyloid fiber formation through asymptotic analysis. *J. Phys. Chem. B* **2012**, *116*, 6611-6617.

(25) Arosio, P.; Vendruscolo, M.; Dobson, C. M.; Knowles, T. P. Chemical kinetics for drug discovery to combat protein aggregation diseases. *Trends Pharmacol. Sci.* **2014**, *35*, 127-135.

(26) Librizzi, F.; Carrotta, R.; Spigolon, D.; Bulone, D.; San Biagio, P. L. α-Casein inhibits insulin amyloid formation by preventing the onset of secondary nucleation processes. *J. Phys. Chem. Lett.* **2014**, *5*, 3043-3048.

(27) Sidhu, A.; Segers-Nolten, I.; Subramaniam, V. Solution conditions define morphological homogeneity of α-synuclein fibrils. *Biochim. Biophys. Acta.* **2014**, *1844*, 2127-2134.

(28) Groenning, M. Binding mode of Thioflavin T and other molecular probes in the context of amyloid fibrils-current status. *J. Chem. Biol.* **2010**, *3*, 1-18.

(29) Knowles, T. P.; Vendruscolo, M.; Dobson, C. M. The amyloid state and its association with protein misfolding diseases. *Nat. Rev. Mol. Cell. Biol.* **2014**, *15*, 384-396.

(30) Cohen, S. I.; Vendruscolo, M.; Welland, M. E.; Dobson, C. M.; Terentjev, E. M.; Knowles, T. P. Nucleated polymerization with secondary pathways. I. Time evolution of the principal moments. *J. Chem. Phys.* **2011**, *135*, 065105.

(31) Giehm, L.; Lorenzen, N.; Otzen, D. E. Assays for α-synuclein aggregation. *Methods* **2011**, *53*, 295-305.

(32) Serpell, L. C.; Berriman, J.; Jakes, R.; Goedert, M.; Crowther, R. A. Fiber diffraction of synthetic α-synuclein filaments shows amyloid-like cross-beta conformation. *Proc. Natl. Acad. Sci. U S A* **2000**, *97*, 4897-4902.

(33) Xue, W. F.; Radford, S. E. An imaging and systems modeling approach to fibril breakage enables prediction of amyloid behavior. *Biophys. J.* **2013**, *105*, 2811-2819.

TOC GRAPHICS